applied sciences

MDPI

Article

Introduction of Internal Circulation-Based Cooling Methods and Green Coolants in Milling via Cutting Tool and Tooling Design

Ilia Radchenko [1], Wataru Takahashi [2], Hidebumi Takahashi [2], Taro Abe [2] and Hiroyuki Sasahara [1,*]

[1] Department of Mechanical Systems Engineering, Tokyo University of Agriculture and Technology, 2-24-16 Naka-Cho, Koganei-shi 184-8588, Tokyo, Japan; s217827t@st.go.tuat.ac.jp
[2] Metalworking Solutions Company, Mitsubishi Materials Corporation, 1-600 Kitabukuro-Cho, Omiya-ku, Saitama-shi 330-8508, Saitama, Japan; wtakahas@mmc.co.jp (W.T.); htkhs@mmc.co.jp (H.T.); t-abe@mmc.co.jp (T.A.)
* Correspondence: sasahara@cc.tuat.ac.jp; Tel.: +81-42-388-7240

Featured Application: The results of the following design investigation can be used in the field of machining, particularly when developing new types of cutting tools and tooling.

Abstract: This paper describes the process of the design and verification of a milling tool and tooling that may contribute to the renouncement of the flood cooling method when mineral oils and oil-in-water emulsions are used as coolants. The proposed solutions are based on the idea of coolant supply in internal channels created inside of a cutting tool. As an alternative to the aforementioned mineral oil-based coolants, liquids with higher cooling efficiency and environmental friendliness (green coolants) were considered. Given coolants' possible lack of lubricating properties and negative (corrosive, etc.) influence on a machine tool's units, tooling delivers these coolants to the cutting tool and bypasses the standard machine tool's supply system. The geometry of the milling tool (a cutting insert with an internal channel) was tested in the framework of a stress simulation. To perform it, cutting force components F_z, F_y, and F_x were determined empirically and then applied to the simulated area of contact between the tool and the workpiece. Based on the obtained principal stress values P_1, P_2, and P_3, the factor of safety was calculated with the *Mohr–Coulomb*, $P_{1\ max}$, and $P_{3\ min}$ failure criteria. The proposed milling tool, equipped with a novel type of labyrinth seal with no friction between its components, was experimentally tested to confirm its ability to maintain leak-tightness at different values of spindle speed (200~2000 rpm) and coolant supply volume (1.0~10.0 L/min). Based on the results of the stress simulation and the leak-tightness experiment, conclusions were drawn about further modernization and utilization prospects of the proposed milling tool and tooling design.

Keywords: machining; milling; cutting tool; tooling; internal circulation; stress test; labyrinth seal

Citation: Radchenko, I.; Takahashi, W.; Takahashi, H.; Abe, T.; Sasahara, H. Introduction of Internal Circulation-Based Cooling Methods and Green Coolants in Milling via Cutting Tool and Tooling Design. *Appl. Sci.* **2024**, *14*, 1379. https://doi.org/10.3390/app14041379

Academic Editors: Roberto Zivieri and Lei Wang

Received: 13 November 2023
Revised: 5 February 2024
Accepted: 6 February 2024
Published: 7 February 2024

1. Introduction

The cutting process represents a consistent removal of a machined material's layers. The deformation is always accompanied by heat generation. The heat generation, together with the resulting friction forces, increases the temperature of a cutting tool at the point of its contact with a workpiece [1]. The high temperature, in turn, negatively affects the properties of a utilized tool material [2], As a consequence, it provokes wear, which reduces the tool life.

The most common way to counteract the above negative factors is the utilization of coolants, often pure mineral oils or oil-in-water emulsions [3]. When turning, milling, etc., the external coolant supply reduces the temperature in the cutting zone along with the friction forces [4], thus positively affecting the tool life.

Traditionally, the external supply has been organized by flooding when coolant is delivered to the cutting tool in large volumes and at low pressure. Mechanically, the supply

is delivered through special hoses, plastic nozzles, metal tubes, or directly through the spindle to the rake and flank faces of a cutting tool or to the cutting zone as a whole. Continuous improvements in the machining field have led to the introduction of other external supply methods. For example, coolant supply under high pressure (2.0 to 7.0 MPa) and the MQL (minimum quantity lubrication, coolant mixed with compressed air and supplied in small volumes) technique can be cited. The main advantage of those, in comparison with flooding, is better penetration into the high-temperature region with often a smaller coolant volume used [5].

Nevertheless, the main problem of the external supply is the inability of the coolant to directly reach the contact point between the tool and the workpiece (Figure 1a). In addition, externally supplied coolants tend to lose effectiveness as cutting speed increases (Figure 1b). Simultaneously, mineral oil-based coolants used for the external supply are often hazardous to the environment and operators' health and require disposal [6].

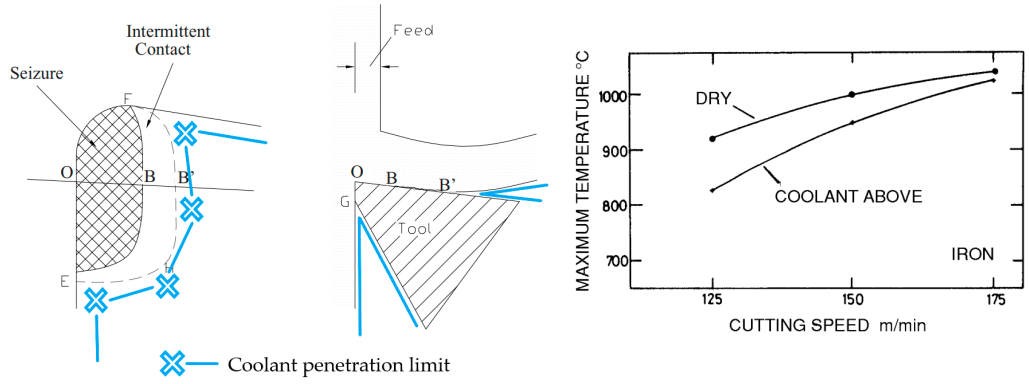

(**a**) (**b**)

Figure 1. External supply coolant penetration (**a**) and efficiency (**b**) issues [7].

To overcome the external supply disadvantages, researchers have proposed alternative ways to deliver coolants to the cutting zone. One of those includes an internal supply, where coolant is delivered exclusively inside the tool through a closed circuit [8–10]. Yet another option is combined supply, where coolant is simultaneously fed inside the tool and to its contact point with the workpiece via separate internal and external circuits [11].

In addition to the alternative supply options, alternative coolants have been proposed to solve the problems of mineral oils and oil-in-water emulsions. These include solutions of vegetable origin (coconut oil, sunflower oil, etc.) [12] and gases supplied at low (~−20 °C, air [13]) and cryogenic temperatures (~−190 °C, nitrogen [14]).

According to the studies' results for turning, the utilization of alternative supply options together with alternative coolants provides better temperature, surface quality, tool life, and environmental performance compared to flooding and dry cutting. This, combined with recent advances in tool design (additive manufacturing [15]), has led to a significant increase in the number of relevant publications since 2010 (Figure 2).

However, for milling, there are fewer works addressing the same topic. One possible reason is the complexity of organizing the delivery of the alternative coolant to the rotating tool. At the same time, standard supply systems of milling machine tools (designed to work with mineral oils and their emulsions) cannot be used with alternative coolants. This is due to the risk of damage to the systems' elements because of low temperatures, corrosion, etc. (especially, when the system supports the spindle-through supply).

As a result, milling lags behind turning both in variations of alternative supply and in the introduction of alternative coolants. In manufacturing environments, milling operations are still often accompanied by flooding with mineral oil-based coolants.

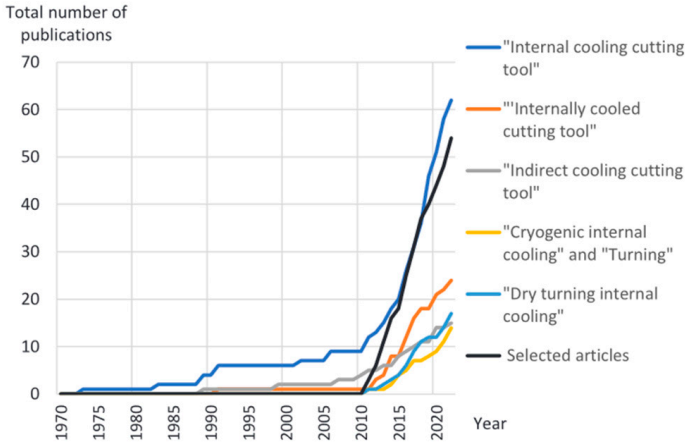

Figure 2. Number of alternative supply-related papers on turning [16].

Previously, the authors proposed variations of the alternative coolant supply realized through the internal and combined schemes (Figure 3). The novel criteria were the channel geometry inside the cutting insert and the use of a single circuit for simultaneous internal and external coolant feed (combined scheme). In turning tests with SUS304 stainless steel, both schemes achieved a small decrease in the contact point temperature and significantly reduced the heat distribution inside the cutting insert body. This ultimately had a positive effect on tool life, tending to strengthen with an increase in cutting speed. The tests were carried out with 4% oil-in-water emulsion with a flow rate of ~0.7 L/min [17].

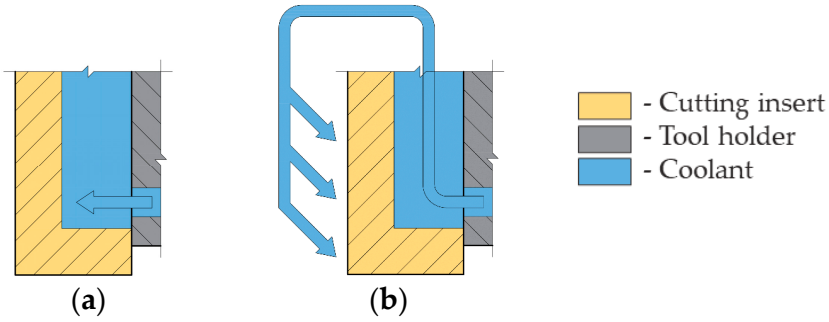

Figure 3. Internal (**a**) and combined (**b**) coolant supply schemes.

The above internal and combined schemes can be introduced to milling as coolant supply options to substitute flooding. Additionally, it reduces the aforementioned lag behind turning in the adoption of alternative supply methods. At the same time, the schemes can be used together with alternative coolants. The problem of organizing their supply to the rotating tool can be solved by designing specialized tooling. The tooling should meet the requirement of bypassing the machine tool's standard supply system, as well as take into account the properties of an alternative coolant being utilized.

Therefore, this study aims to develop a milling tool that realizes the alternative internal and combined supply schemes. In parallel, a tooling method is designed to allow the use of an alternative coolant and its delivery to bypass the machine tool's standard supply system.

2. Materials and Methods of Determining the Design of the Proposed Solutions

2.1. Selection of an Alternative Coolant

The key stage, which directly influences further design decisions, is the determination of potential alternative coolants. The selected variant must overcome the disadvantages of mineral oil-based solutions. At the same time, it should not be inferior to them in cooling efficiency and, ideally, should be affordable in operation. The previously mentioned vegetable oil-based coolants, despite their environmental friendliness, still require disposal

procedures (though less complex in comparison with mineral oil-based solutions). Gas, namely, nitrogen (in liquid state), is free of this disadvantage and demonstrates high cooling efficiency. However, the organization of its supply to the tool, due to the extremely low operating temperature, is a non-trivial and expensive task.

As a result, pure water, which has better thermal conductivity than mineral and vegetable oils, was chosen as the alternative coolant [18]. It should be noted that water is the base of most emulsions. Often, oil concentration in those does not exceed ~2–10%. Due to this fact, the properties of emulsions, unlike those of pure oils, differ little from those of water (Table 1). Nevertheless, the most important aspects in which water is superior are environmental friendliness and low cost of operation. Considering the current green trend in machining, these factors have become crucial for selection. Water, however, is an alternative coolant that, due to its properties, cannot be fed through a machine tool's standard supply system. These properties (low lubrication capacity and risk of corrosion) were taken into account when the tooling was designed.

Table 1. Oil-in-water emulsion and water properties in comparison.

Coolant	Property	
	Density at 20 °C, kg/m^3	**Viscosity at 20 °C, mPa s**
6% Oil-in-water emulsion [19]	~995.8	1.1
Pure water	~998.0	1.0 L

2.2. Milling Tool Design

For the cutting tool, the necessity of implementing the internal and combined coolant supply schemes was taken into account. This made the presence of internal channels in the tool design mandatory. To simplify the overall manufacturing process, the idea of a modular end mill was chosen. The end mill had to consist of a shank, a replaceable tool holder, and two cartridges equipped with cutting inserts.

The shank design was determined by the planned features and dimensions for the tooling. The HSK63 system was selected to install the shank into the machine spindle. The tool holder (1) was centered on the shank axis (2) and secured from slippage with two retaining keys (3) and the central locking bolt (4) (Figure 4). The holder was designed to carry two cartridges. Those were based on commercially available Mitsubishi Materials PSSN 16CA12 cartridges equipped with SNMA 120408 cutting inserts made of uncoated UTi20T carbide. The final geometric parameters of the end mill are summarized in Table 2.

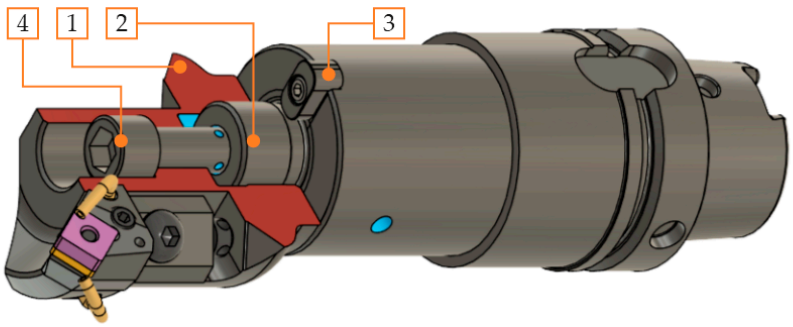

Figure 4. Shank and tool holder connection.

Table 2. End mill geometric parameters.

Parameter	Value	Notes	Cutting Angle Explanation
Full length *L*, mm	200.0	From the spindle to the insert tip	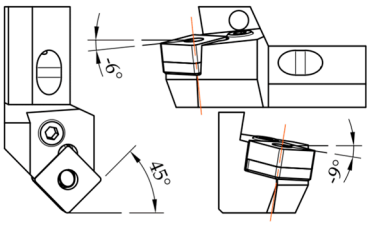
Mill diameter *D*, mm	63.0	Between the inserts tips	
Number of teeth *z*	2	= number of cartridges	
Rake angle, °	−6.0	Angles explained with an unmodified PSSN cartridge	
Radial rake angle, °	−9.0		
Lead angle, °	45.0		

2.3. Coolant Supply Channels

To implement the internal and combined coolant supply schemes, the end mill shank, tool holder, cartridges, and cutting inserts were equipped with internal channels. Their shape and location were determined to ensure sufficient flow capacity and relative simplicity of manufacture. The shank was equipped with three drilled channels (Figure 5a). The central channel (1) with a diameter of 10.2 mm was positioned on the tool rotation axis. Two side channels (2, 3) of 6.0 mm diameter, perpendicular to the axis, were created to connect the central one with the coolant circuit of the tooling. The locking bolt had holes (4) to pass the coolant further through the tool holder's channels.

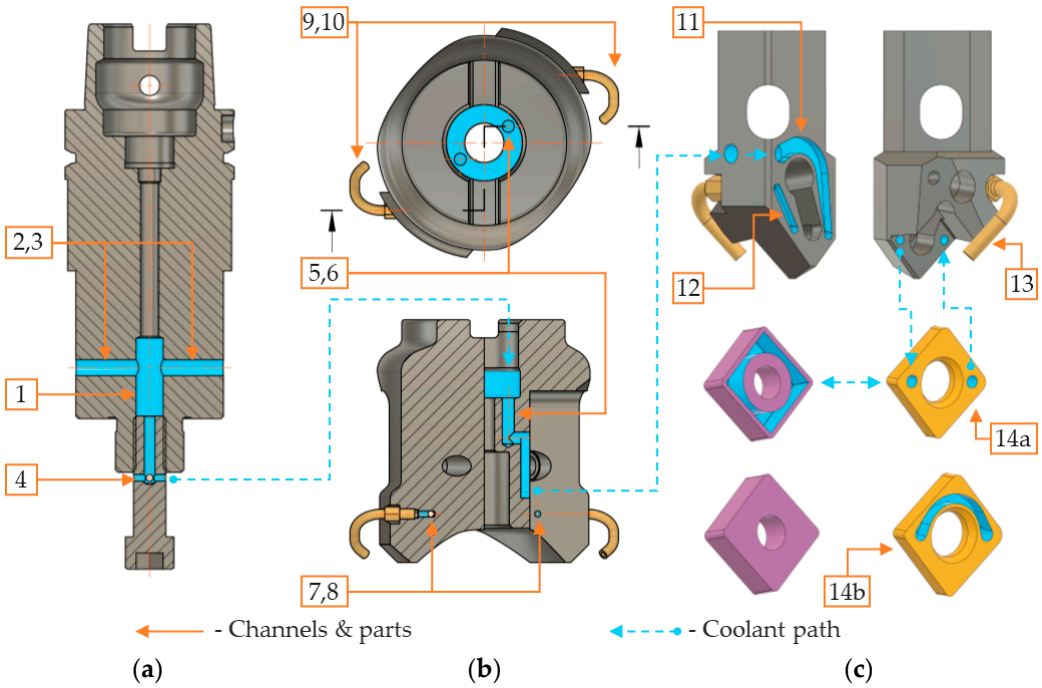

Figure 5. Tool shank (**a**), tool holder (**b**), and cartridge (insert + carbide plate) (**c**) supply channels.

Two of the holder channels (5, 6) were manufactured by drilling and milling to merge with the cartridges. Another two (7, 8) provided external coolant supply to the flank faces of the cutting inserts through the designated pipes (9, 10) (Figure 5b). Sealing of the channels' machined sections occurs when the cartridges are installed in their seats.

The cartridges were equipped with channels of complex configuration. The first channel (11) is to supply coolant to the cutting insert. After that, via the second channel (12), coolant may be discharged from the cutting zone or forwarded to the insert's rake face through the pipe (13) (Figure 5c). From this point, the aforementioned channels (7, 8) of the tool holder are begun as well.

The geometry of the cutting insert channel was determined by two factors. First, the maximum thermal efficiency of the supplied coolant had to be ensured. Second, there had to be no risk of the insert body experiencing catastrophic failure caused by the cutting loads (verified by the stress simulation, described in Section 2.8).

The selected cartridges were equipped with a carbide plate installed under the cutting insert. This plate was modified in two ways. For the tool to function as the proposed internal and combined supply schemes, inlet and outlet holes were created in the body of the plate (14a). The position of those coincided with the cutting insert channel. To supply coolant only externally, an insert with no channel is meant to be used. Therefore, to keep the coolant flow, a bypass channel was created in the carbide plate (14b).

2.4. Milling Tooling

The milling tooling had to supply alternative coolant (water) bypassing the standard supply system and any key components of the machine tool. Consequently, the alternative coolant supply line had to be connected directly to the tooling housing. This led to the necessity of keeping the housing in a static position, even when the tool is rotating. Accordingly, the tooling was developed with the inclusion of a bearing unit and seals capable of maintaining leak-tightness between the static and rotating parts. At the same time, due to the unsatisfactory lubricating properties of water, it was necessary to eliminate or minimize the friction occurring between the parts' surfaces to prevent the tooling from jamming.

The shape of the tooling housing was determined by several factors:

- The type, size, and number of bearings to be used;
- The type of fittings planned for connection to the alternative coolant supply line;
- The type of seal to be used at the interface between the static and rotating parts;
- The need to ensure sufficient ease of fabrication, assembly, and maintenance;
- The dimensions of the tooling had to allow its use within the tool magazine.

Two NSK 6811 DDU (NSK, Ann Arbor, MI, USA) [20] single-row ball bearings were selected, equipped with a contact seal between the outer and inner rings. The maximum rotation speed determined by the manufacturer was 4800 rpm ($V_{c\ max}$ = 950 m/min for the cutter diameter of 63.0 mm). The bearings were installed in the upper part of the tooling housing (Figure 6).

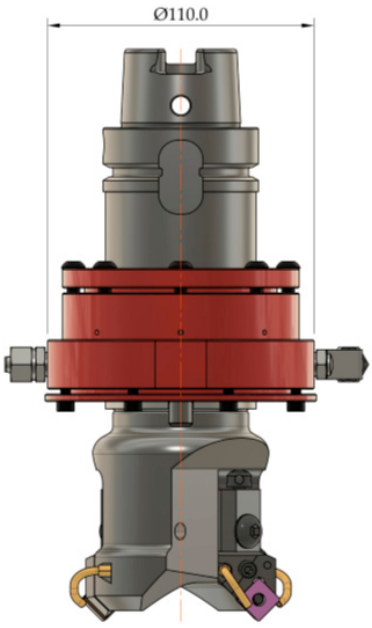

Figure 6. Assembled tooling.

For connection with the alternative coolant (water) supply line, two holes with an R_c 1/8 thread were placed coaxially in the tooling housing, allowing a uniform supply from both sides through fittings. The convenience of fabrication, assembly/disassembly, and maintenance was provided by dividing the tooling housing into upper, middle, and lower parts. The parts were fixed relative to each other with M4 and M5 screws. The maximum diameter of the tooling without the fittings was 110.0 mm (Figure 6) (with the common diameter limitation of 120.0 mm for the tool magazine).

2.5. Milling Tooling Seal

To minimize friction and avoid jamming, the option of sealing the tooling with gland-like rings or contact washers was not considered. Labyrinth seals, variations of which are most often used in gas turbine equipment [21], had a design suitable for the specified conditions. The key feature of labyrinth seals is the absence of contact between the rotating and static parts. Nevertheless, under the conditions of limited tooling dimensions, manufacturing sealing chambers with a traditional four-corner shape is problematic due to the need for specialized tools. Therefore, the authors decided to use a new, triangular chamber geometry (Figure 7), which can be produced with commonly available cutters. The fully assembled seal consists of three rotating (1, 2, 3) and one static part (4) with a minimum radial clearance of 0.25 mm. The parts form the upper (5) and lower (6) sealing chamber sets. As the coolant passes through the chambers, its pressure decreases to the atmospheric level, which should stop the flow and prevent or minimize leakage. As a precautionary measure, both sets of chambers can discharge excess coolant through the special holes in the tooling housing immediately after the upper set (7) and through the gap between the rotating and static parts (8) immediately after the lower set. For the designed tooling, taking into account the limited maximum diameter, the number of chambers was restricted to six.

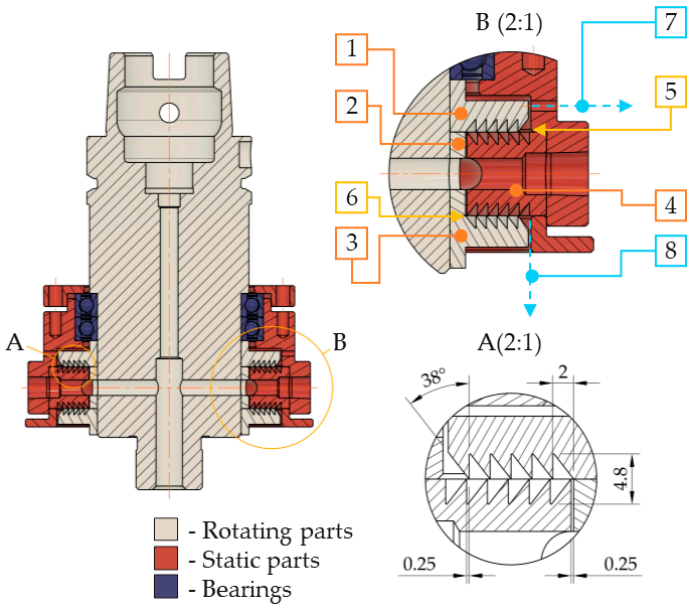

Figure 7. Tooling rotation scheme and labyrinth seal geometry (A and B are enlarged sections).

2.6. Utilized Materials

The tooling component materials were selected based on the properties of the alternative coolant used. The tooling housing parts were made of stainless steel SUS304 (AISI304 analog) capable of resisting corrosion [22]. The seal material was polyoxymethylene (POM), a structural plastic that maintains high geometric accuracy and has a low friction coefficient. The lower rotating part of the seal was made of SUS304 to accommodate the retaining keys of the end mill shank.

2.7. Verification of the Selected Designs for the Proposed Solutions

The performance and reliability of the developed solutions, namely, the insert with the circulation channel and the tooling equipped with the labyrinth seal, were confirmed through simulation and experiments. SolidWorks 2019 software with SolidWorks Simulation add-on utilizing finite element analysis (FEA) was chosen as the simulation platform. The base for the experiments was a three-axis machining center MAZAK FJV-250 equipped with a standard contour of external coolant supply to the cutting zone, including a GRUNDFOS CRK2-180 AMA AUUV pump (GRUNDFOS, Bjerringbro, Denmark) with a working pressure of 1.6~0.7 MPa at a flow rate of 16~58 L/min.

2.8. Cutting Insert Stress Simulation

Equipping the cutting insert with the channel leads to the formation of rake and flank walls (Figure 8). The smaller thickness of the rake wall improves heat dissipation through the channel since most of it comes from the highest temperature zone, located on the insert's rake face. The flank wall perceives the main cutting force component, acting perpendicularly on the rake face. Based on the Mitsubishi Materials specifications, the flank wall thickness was set as 0.75 mm. The rake wall thickness (Figure 8, variable *H*) was determined by simulating the application of the cutting force to the insert. Values ranging from 0.95 to 0.55 mm in 0.05 mm increments were selected as possible thickness H. The stress simulation logic corresponded to a linear static analysis. A scheme of the simulated milling process is shown in Figure 9. SUS304 stainless steel was simulated as the machined material.

The cutting insert model was mounted on the carbide plate model attached to the cartridge model body, as shown in Figure 10. The carbide plate and cartridge models were assumed to be absolutely solid, without regard to the characteristics of the materials or any influence on the final stress simulation results. The tested insert material's physical properties are provided in Table 3. The models were fixed through the back surface of the cartridge to simulate its installation in the tool holder.

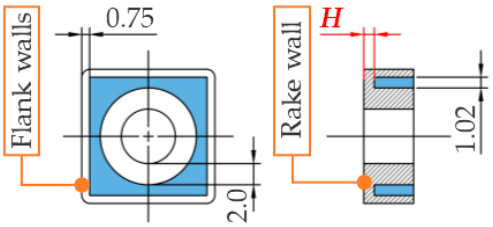

Figure 8. Insert rake and flank walls.

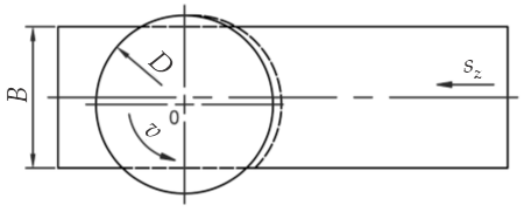

Figure 9. Milling process scheme.

Table 3. Tested insert material's physical properties.

Parameter	Value
Elastic modulus, GPa	630.0
Mass density, g/cm^3	14.9
Tensile strength, GPa	1.2
Compressive strength, GPa	5.7
Yield strength, GPa	1.1

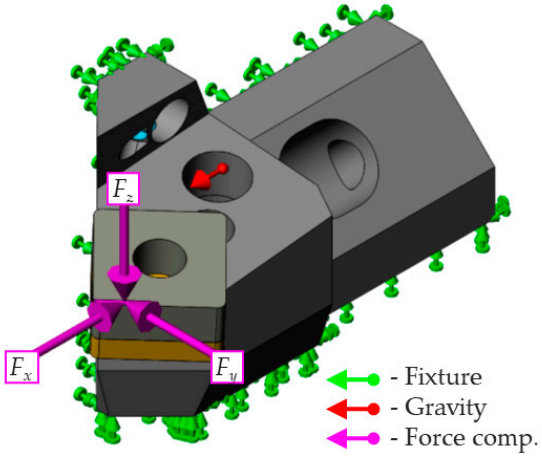

Figure 10. Stress simulation setup.

The cutting force was divided into three components, F_z, F_x, and F_y. As an additional condition, gravity was applied in the direction opposite to the component F_x. The width of the component application area corresponded to the simulated value of the tool feed rate, and the height of the area was equal to the depth of cut. The value of the cutting force component F_z was calculated using the following equation [23]:

$$F_z = \frac{10C_p t^x s_z^y B^n z}{D^q n^w} K_{mp}, \quad (1)$$

where C_p, x, y, q, and w are coefficients determined by the tool design and machined material.

t is the depth of cut in mm.
s_z is the tool feed rate in mm/tooth.
B is the cutting width of 50 mm within the adopted milling process scheme.
n is the spindle speed in rpm Under the conditions of machining stainless steel, the speed coefficient w was 0, which equated any value of speed to 1.0. Consequently, the spindle speed was not taken into account during the calculation.
K_{mp} is the coefficient of the machined material's characteristics, determined by the following equation:

$$K_{mp} = \left(\frac{\sigma^B}{750}\right)^{0.3}, \quad (2)$$

where σ^B is the tensile strength of the machined material, equating to 505 MPa for SUS304 (AISI304 [24]).

The cutting force components F_x and F_y for the utilized mill type were calculated using the equations below:

$$F_x = 0.55F_z \quad (3)$$

$$F_y = 0.40F_z \quad (4)$$

Determination of the values of the components F_z, F_x, and F_y was carried out based on three variants of the tool feed rate s_z and three variants of the depth of cut t, through the combination of which nine cutting modes were obtained. The obtained cutting modes with the calculated component values are shown in Table 4.

The cutting insert material is similar in physical characteristics to tungsten carbide and belongs to the brittle category. Consequently, when testing the front wall thickness H variants, the stresses on the insert were evaluated based on the obtained maximum and minimum values of the principal stresses P_1, P_2, and P_3. Subsequently, the obtained values were used to calculate the factor of safety. The factor of safety was determined by using three failure criteria: (a) *Mohr–Coulomb* [25], (b) limit on $P_{1\ max}$, and (c) limit on $P_{3\ min}$.

The factor of safety values for the $P_{1\ max}$ and $P_{3\ min}$ limits were calculated utilizing the following equations:

$$FoS_{P_{1\ max}} = \frac{\sigma_{tens}}{P_{1\ max}}, \quad (5)$$

where $P_{1\ max}$ is the maximum value of principal stress P_1

$$FoS_{P_{3\ min}} = \frac{\sigma_{comp}}{P_{3\ min}} \quad (6)$$

where $P_{3\ min}$ is the minimum value of principal stress P_3.

Only the values of thickness H that excluded the risk of insert breakage and had factor of safety values greater than 2.0 were considered reliable ones.

Table 4. Cutting modes (1–9) and force component values.

s_z = 0.2 mm/tooth | depth of cut		
(1) 1.0 mm	**(2) 2.0 mm**	**(3) 4.0 mm**
$F_z = 471N$ $F_x = 259N$ $F_y = 188N$	$F_z = 892N$ $F_x = 491N$ $F_y = 357N$	$F_z = 1688N$, $F_x = 928N$, $F_y = 675N$.
s_z = 0.4 mm/tooth | depth of cut		
(4) 1.0 mm	**(5) 2.0 mm**	**(6) 4.0 mm**
$F_z = 810N$ $F_x = 445N$ $F_y = 324N$	$F_z = 1532N$ $F_x = 842N$ $F_y = 613N$	$F_z = 2898N$ $F_x = 1594N$ $F_y = 1159N$
s_z = 0.6 mm/tooth | depth of cut		
(7) 1.0 mm	**(8) 2.0 mm**	**(9) 4.0 mm**
$F_z = 1111N$ $F_x = 611N$ $F_y = 444N$	$F_z = 2101N$ $F_x = 1156N$ $F_y = 841N$	$F_z = 3976N$ $F_x = 2187N$ $F_y = 1591N$

2.9. Checking the Labyrinth Seal

The labyrinth seal had clearance (0.25 mm) between the parts necessary to eliminate friction. This peculiarity became the main reason for conducting an experiment to determine the seal's leak-tightness. Within the framework of this work, due to the design's novelty—the absence of a ready-made alternative coolant (water) supply contour—as well as due to the machining center being involved in several parallel studies, the labyrinth seal was tested with the use of Daphne Alphacool EX-1 5% oil-in-water emulsion at 20 °C. The tooling, mounted on the tool shank, was installed in the spindle and connected to the machining center's standard coolant supply system through two fittings (1, 2), as shown in Figure 11. The connection was made by oil-resistant hoses with an inner diameter of 6.0 mm. To control the pressure and volume of the supplied coolant, we used a GPI S051 flow sensor ((3), installed at the machine pump outlet) and an SMC PPA102 electronic manometer (4) with a measuring range of −10~+100 kPa. The supplied coolant volume was regulated by the valve installed at the flow sensor. The valve (5) installed between the outlet of the standard supply system and the hoses was fully open during the experiment.

A labyrinth seal check was performed at coolant volume rates of 1.0 to 10.0 L/min in 1.0 L/min increments and spindle speeds of 0 to 2000 rpm in 200 rpm increments. The results were evaluated on the basis of (a) the presence or absence of coolant leakage through the tooling to the center hole of the shank (6) and (b) the presence or absence of visual leakage through the previously mentioned special holes in the tooling housing immediately after the upper set (7) and through the gap between the parts immediately after the lower set (8) of sealing chambers. In order to simplify visual observation of coolant leakage, the inspection was carried out without the tool holder and cartridges installed.

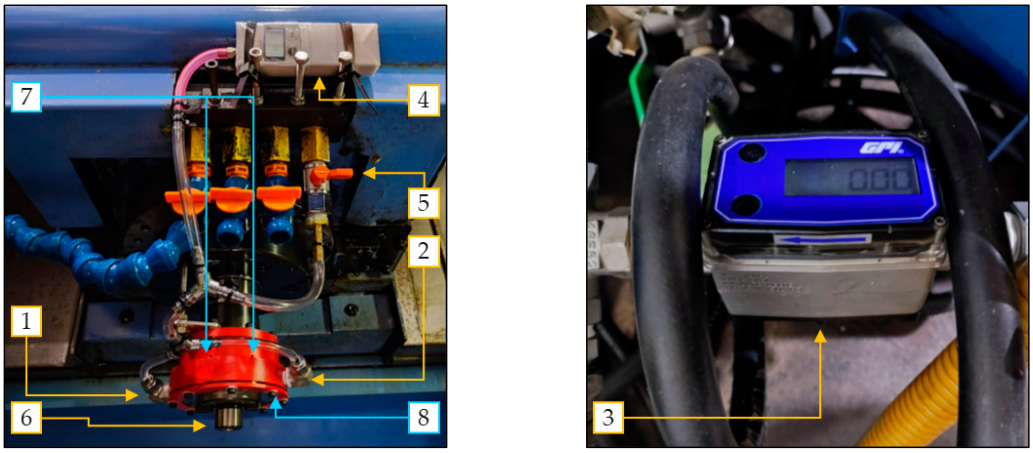

Figure 11. Labyrinth seal check setup.

3. Results of the Design Verification of the Proposed Solutions

3.1. Cutting Insert's Factor of Safety

The maximum and minimum values of principal stresses P_1, P_2, and P_3 obtained as a result of the stress simulation are provided for all selected cutting modes in Figure 12, with a visual example of the principal stress effect on the insert body shown in Figure 13.

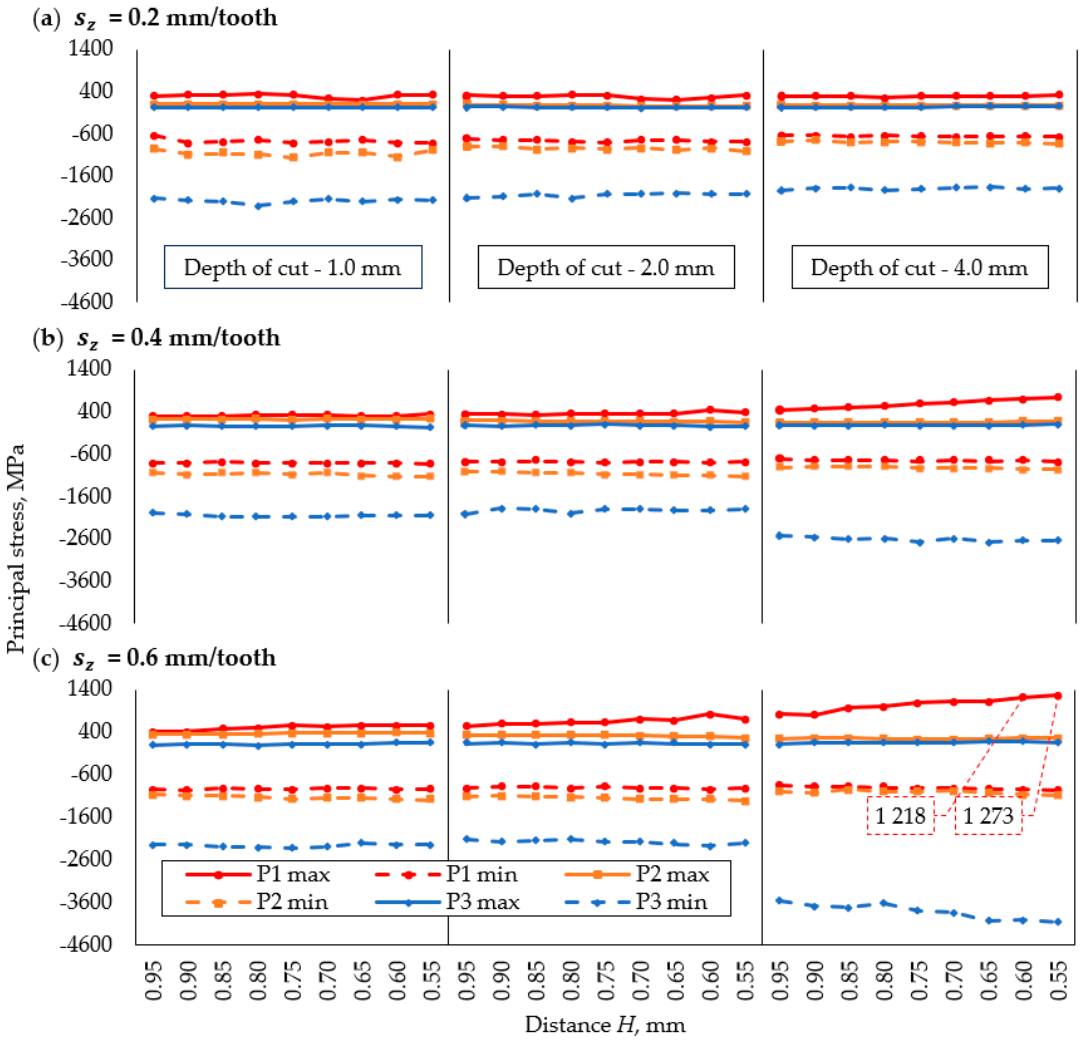

Figure 12. Principal stress values, obtained from the simulation.

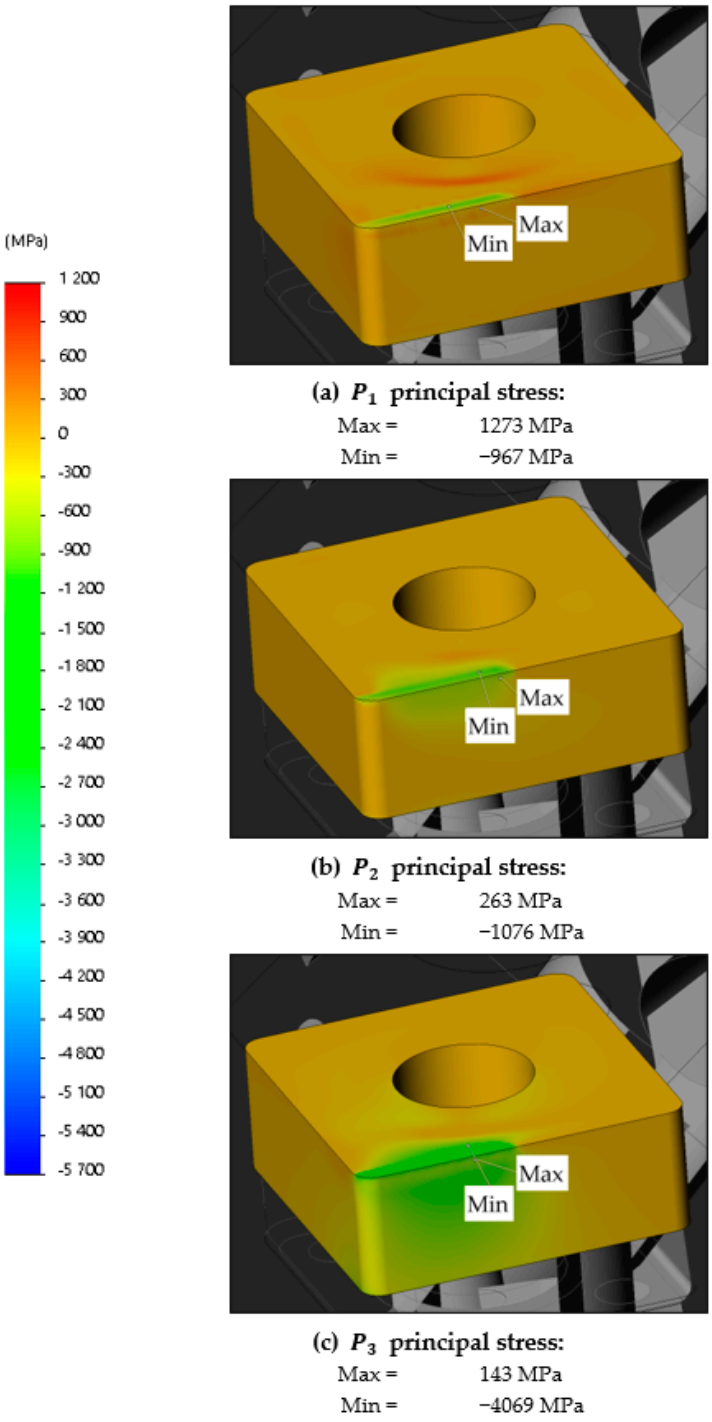

Figure 13. Principal stress effect on the insert body.

The possibility of catastrophic failure as stress $P_{1\ max}$ exceeded the tensile strength limit of the insert material (Table 3) existed only at the 0.6 mm/tooth tool feed rate and the 4.0 mm depth of cut for the rake wall thickness H equal to 0.60 and 0.55 mm (instances exceeding the limit values of $P_{1\ max}$ are noted in Figure 12c). Based on the graphs, it is possible to observe a pronounced effect of the feed rate on the growth of the principal stress values $P_{1\ max}$ and $P_{3\ min}$ at the 4.0 mm depth of cut, which is associated with the largest size of the simulated contact area between the tool and the workpiece.

The results of determining the cutting insert's factor of safety at different front wall thicknesses H using the three previously selected failure criteria (*Mohr–Coulomb*, $FoS_{P_{1\ max}}$, $FoS_{P_{3\ min}}$) are shown in Figure 14. The dotted line indicates the adopted minimum factor of

safety, equal to 2.0. For the 0.4 and 0.6 mm/tooth tool feed rates, the factor of safety tended to decrease with increasing depth of cut. The final evaluation of the results was carried out using the unified Table 5.

The factor of safety for each tested rake wall thickness H had two states according to the *Mohr–Coulomb* criterion and three states according to the combined $FoS_{P_{1\ max}}$ and $FoS_{P_{3\ min}}$ criteria. Despite the difference in the criteria calculation methodology, the obtained test results are consistent (assuming only H thicknesses with factor of safety values greater than 2.0 were accepted as reliable).

At the 0.2 mm/tooth tool feed rate and all depths of cut (1.0, 2.0, 4.0 mm), the factor of safety exceeded the value of 2.0, which allowed the minimum thickness H of the insert's rake wall equal to 0.55 mm to be used. At the same time, for the 0.4 mm/tooth tool feed rate, the use of the thickness H of 0.55 mm was possible only for the 1.0 and 2.0 mm depths of cut. For the 4.0 mm depth of cut, the minimum possible thickness H was 0.75 mm. At the 0.6 mm/tooth tool feed rate, the thickness H of 0.55 mm was only possible at the 1.0 mm depth of cut. For the 2.0 mm depth of cut, the H value needed to be at least 0.9 mm. For the 4.0 mm depth of cut, no H values showed a sufficient factor of safety under the stress simulation conditions.

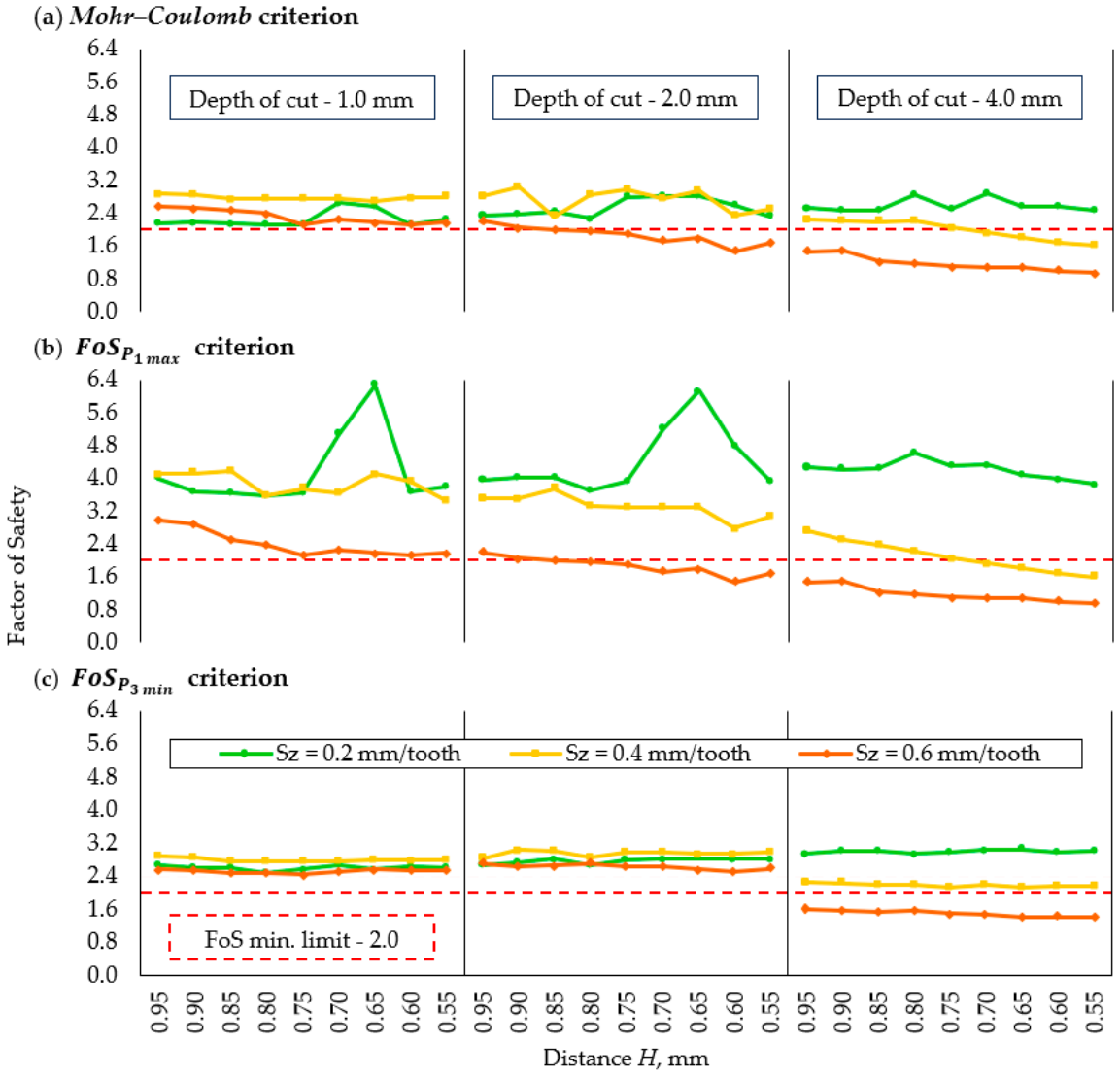

Figure 14. Factor of safety results, determined from the simulation.

Table 5. Factor of safety final result evaluation.

s_z, mm/Tooth	Depth of Cut, mm	Distance *H*, mm								
		0.95	0.90	0.85	0.80	0.75	0.70	0.65	0.60	0.55
(a) *Mohr–Coulomb* criterion										
0.2	1.0	◆	◆	◆	◆	◆	◆	◆	◆	◆
	2.0	◆	◆	◆	◆	◆	◆	◆	◆	◆
	4.0	◆	◆	◆	◆	◆	◆	◆	◆	◆
0.4	1.0	◆	◆	◆	◆	◆	◆	◆	◆	◆
	2.0	◆	◆	◆	◆	◆	◆	◆	◆	◆
	4.0	◆	◆	◆	◆	◆	⦿	⦿	⦿	⦿
0.6	1.0	◆	◆	◆	◆	◆	◆	◆	◆	◆
	2.0	◆	◆	⦿	⦿	⦿	⦿	⦿	⦿	⦿
	4.0	⦿	⦿	⦿	⦿	⦿	⦿	⦿	⦿	⦿
Legend: ◆—Factor of safety > 2.0, ⦿—Factor of safety < 2.0										
(b) $FoS_{P_{1max}}$ and $FoS_{P_{3min}}$ criteria										
0.2	1.0	◆	◆	◆	◆	◆	◆	◆	◆	◆
	2.0	◆	◆	◆	◆	◆	◆	◆	◆	◆
	4.0	◆	◆	◆	◆	◆	◆	◆	◆	◆
0.4	1.0	◆	◆	◆	◆	◆	◆	◆	◆	◆
	2.0	◆	◆	◆	◆	◆	◆	◆	◆	◆
	4.0	◆	◆	◆	◆	◆	◀	◀	◀	◀
0.6	1.0	◆	◆	◆	◆	◆	◆	◆	◆	◆
	2.0	◆	◆	◀	◀	◀	◀	◀	◀	◀
	4.0	⦿	⦿	⦿	⦿	⦿	⦿	⦿	⦿	⦿
Legend: ◆—$FoS_{P_{1\ max}} >$ 2.0 & $FoS_{P_{3\ min}} >$ 2.0, ◀—$FoS_{P_{1\ max}} <$ 2.0 & $FoS_{P_{3\ min}} >$ 2.0, ⦿—$FoS_{P_{1\ max}} <$ 2.0 & $FoS_{P_{3\ min}} <$ 2.0										

3.2. Labyrinth Seal Check Results

The results of checking the tooling labyrinth seal at spindle speeds of 0 to 2000 rpm and coolant supply volumes of 1.0 to 10.0 L/min (with the coolant pressure in kPa corresponding to each volume value) are shown in Figure 15.

During the check, three conditions of the tooling were detected when the spindle speed and coolant volume were changed. In condition (a), the labyrinth seal did not perform its function, and at the same time, no coolant flowed through the center hole of the shank. In condition (b), the seal still did not perform its function, but coolant flowed through the center hole. In condition (c), the seal was functioning correctly and there was coolant flow through the shank.

Conditions (a), (b), and (c) did not overlap and appeared sequentially as the spindle speed increased. Increasing the volume of supplied coolant shifted the transition boundaries from one state to another. At a low coolant supply volume (1.0 L/min/7 kPa), the tooling stayed in condition (c) (correct operation) until the spindle speed reached 1400 rpm. With a further increase in speed and constant pressure, the tooling moved to condition (a).

The reason for the transition was the increasing resistance for the coolant to flow from the static tooling piece into the 6.0 mm diameter channels of the rotating shank. If the coolant volume and pressure were insufficient, this led to the coolant being squeezed outward through the labyrinth seal. As the volume of supplied coolant increased, condition (b) appeared between conditions (a) and (c), at which point the created pressure was sufficient to deliver the coolant into the rotating shank, but it exceeded the ability of the labyrinth

seal to maintain leak-tightness. The further increase in the volume of supplied coolant up to 5.0 L/min led to the complete replacement of conditions (c) and (a) by condition (b).

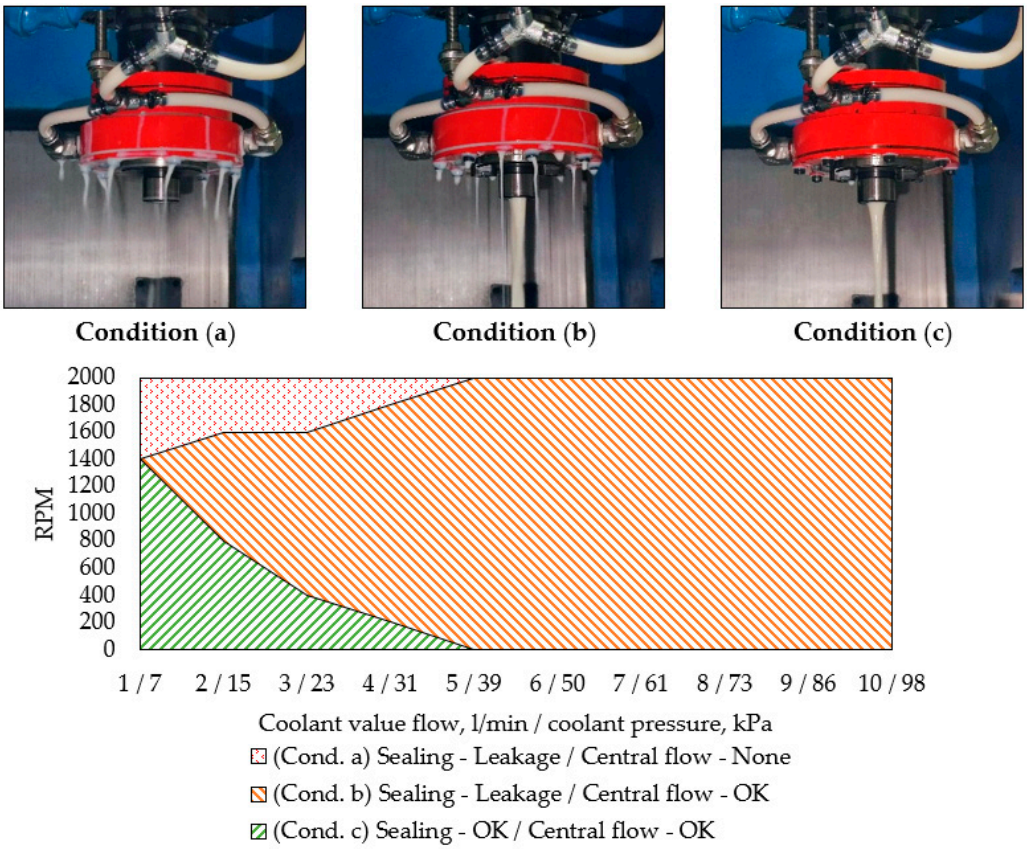

Figure 15. Labyrinth seal check results.

The analysis of the check results showed that the proposed design of the milling tooling and labyrinth seal can provide leak-tightness and coolant supply to the rotating modular end mill at a flow volume of 1.0 L/min with a maximum spindle speed of 1400 rpm. At a 63.0 mm working mill diameter, this spindle speed is equal to a cutting speed of ~275 m/min. With a 3.0 L/min volume, the maximum cutting speed, assuming that the leak-tightness is maintained, is ~80 m/min.

4. Conclusions

The proposed milling tool implements the alternative internal and combined coolant supply schemes and may be of use to substitute the flood cooling method, which is still widespread in milling. At the same time, the designed milling tooling will help to deliver an alternative coolant straight to the tool, omitting the fear of damaging a standard machine tool's supply system.

In the framework of the present design-focused study, the main steps to confirm the reliability of the developed solutions were performed. The cutting insert shape, after adding the channel for the coolant to circulate, was tested to withhold the probable cutting loads. The tooling, namely, its novel labyrinth seal, did undergo leak-tightness investigation.

In general, the study outcome can be considered promising, yet there is always space for improvement to be made in the near future.

First of all, the values of the cutting force components F_z, F_x, and F_y were obtained empirically. Despite the applied calculation strategy being well known, it is desirable to confirm the obtained values experimentally by reproducing the nine utilized cutting modes (Table 4) and by measuring the force data with a dynamometer. If there is a necessity to further change the shape of the insert or its channel by applying thinner walls, a more

complex shape, etc., the current simulation algorithm may be improved for dynamic or time-dependent loads as well.

The tooling and its labyrinth seal may be utilized "as is" if supplying a coolant in small volumes (up to 1.0 L/min with a max. of 1400 rpm) is acceptable. On the other hand, the design can be modified to increase the maximum rotation speed, the coolant volume flow, etc. again by means of special algorithms or simulations. Those may take into account the static and rotating sections' behavior.

As was mentioned in the main text, the initial tooling prototype, though meant to be used with water, was tested with an emulsion. However, the authors do accept the leak-tightness experiment's results as reliable since the difference between the properties of water and the emulsions may be considered not significant (Table 1). Nevertheless, the authors are willing to overcome the reasons for not using water described in Section 2.9.

In addition to the above improvements, a series of milling experiments are planned to investigate how to further evolve the tool and tooling design and to form a fully functioning supply system for not only water but also a wide range of alternative coolants.

Author Contributions: Conceptualization, I.R.; formal analysis, I.R.; investigation, I.R.; methodology, I.R.; validation, I.R., W.T., H.T., T.A. and H.S.; visualization, I.R.; writing—original draft preparation, I.R.; resources, W.T., H.T. and T.A.; funding acquisition, W.T., H.T. and T.A.; supervision, H.S.; writing—review and editing, H.S. All authors have read and agreed to the published version of the manuscript.

Funding: Partial financial support was received from the Japanese Ministry of Education, Culture, Sports, Science, and Technology and from the Mitsubishi Materials Corporation.

Institutional Review Board Statement: Not applicable.

Informed Consent Statement: Not applicable.

Data Availability Statement: The raw data supporting the conclusions of this article will be made available by the authors on request.

Conflicts of Interest: Authors Wataru Takahashi, Hidebumi Takahashi and Taro Abe were employed by the Metalworking Solutions Company, Mitsubishi Materials Corporation. The remaining authors declare that the research was conducted in the absence of any commercial or financial relationships that could be construed as a potential conflict of interest.

References

1. Abukhshim, N.A.; Mativenga, P.T.; Sheikh, M.A. Heat Generation and Temperature Prediction in Metal Cutting: A Review and Implications for High Speed Machining. *Int. J. Mach. Tools Manuf.* **2006**, *46*, 782–800. [CrossRef]
2. Groover, M.P. *Fundamentals of Modern Manufacturing: Materials, Processes, and Systems*, 7th ed.; John Wiley & Sons, Inc.: Hoboken, NJ, USA, 2020; ISBN 978-1-119-49438-6.
3. El Baradie, M.A. Cutting Fluids: Part I. Characterisation. *J. Mater. Process. Technol.* **1996**, *56*, 786–797. [CrossRef]
4. Zheng Yang, K.; Pramanik, A.; Basak, A.K.; Dong, Y.; Prakash, C.; Shankar, S.; Dixit, S.; Kumar, K.; Ivanovich Vatin, N. Application of Coolants during Tool-Based Machining—A Review. *Ain Shams Eng. J.* **2023**, *14*, 101830. [CrossRef]
5. Kui, G.W.A.; Islam, S.; Reddy, M.M.; Khandoker, N.; Chen, V.L.C. Recent Progress and Evolution of Coolant Usages in Conventional Machining Methods: A Comprehensive Review. *Int. J. Adv. Manuf. Technol.* **2022**, *119*, 3–40. [CrossRef] [PubMed]
6. El Baradie, M.A. Cutting Fluids: Part II. Recycling and Clean Machining. *J. Mater. Process. Technol.* **1996**, *56*, 798–806. [CrossRef]
7. Trent, E.M.; Wright, P.K. *Metal Cutting*, 4th ed.; Butterworth-Heinemann: Boston, MA, USA, 2000; ISBN 978-0-7506-7069-2.
8. Sanchez, L.E.D.A.; Neto, R.R.I.; Fragelli, R.L.; Junior, C.E.D.S.; Scalon, V.L. Machining with Internally Cooled Toolholder Using a Phase Change Fluid. *Procedia CIRP* **2016**, *41*, 847–851. [CrossRef]
9. Isik, Y. Using Internally Cooled Cutting Tools in the Machining of Difficult-to-Cut Materials Based on Waspaloy. *Adv. Mech. Eng.* **2016**, *8*, 1687814016647888. [CrossRef]
10. Chiou, R.Y.; Lu, L.; Chen, J.S.J.; North, M.T. Investigation of Dry Machining with Embedded Heat Pipe Cooling by Finite Element Analysis and Experiments. *Int. J. Adv. Manuf. Technol.* **2007**, *31*, 905–914. [CrossRef]
11. Shu, S.; Zhang, Y.; He, Y.; Zhang, H. Design of a Novel Turning Tool Cooled by Combining Circulating Internal Cooling with Spray Cooling for Green Cutting. *J. Adv. Mech. Des. Syst. Manuf.* **2021**, *15*, JAMDSM0003. [CrossRef]
12. Wickramasinghe, K.C.; Sasahara, H.; Rahim, E.A.; Perera, G.I.P. Green Metalworking Fluids for Sustainable Machining Applications: A Review. *J. Clean. Prod.* **2020**, *257*, 120552. [CrossRef]
13. Su, Y.; He, N.; Li, L.; Iqbal, A.; Xiao, M.H.; Xu, S.; Qiu, B.G. Refrigerated Cooling Air Cutting of Difficult-to-Cut Materials. *Int. J. Mach. Tools Manuf.* **2007**, *47*, 927–933. [CrossRef]

14. Hong, S.Y.; Ding, Y. Cooling Approaches and Cutting Temperatures in Cryogenic Machining of Ti-6Al-4V. *Int. J. Mach. Tools Manuf.* **2001**, *41*, 1417–1437. [CrossRef]
15. Anuj Srivathsa, S.S.; Muralidharan, B. Review on 3D Printing Techniques for Cutting Tools with Cooling Channels. *Heliyon* **2023**, *9*, e22557. [CrossRef]
16. Korenkovs, A.; Gerins, E.; Kromanis, A. The Design and Performance of Internally Cooled Cutting Tools for Turning: A Literature Review. *Latv. J. Phys. Tech. Sci.* **2023**, *60*, 73–94. [CrossRef]
17. Radchenko, I.; Takahashi, W.; Takahashi, H.; Sasahara, H. Effects of Internal Coolant Circulation-Based Cooling Schemes on Tool Wear in Turning SUS304 Stainless Steel. *Int. J. Adv. Manuf. Technol.* **2023**, *129*, 3141–3154. [CrossRef]
18. Liquids—Thermal Conductivities. Available online: https://www.engineeringtoolbox.com/thermal-conductivity-liquids-d_1260.html (accessed on 13 November 2023).
19. Sokolović, D.S.; Höflinger, W.; Šečerov Sokolović, R.M.; Sokolović, S.M.; Sakulski, D. Experimental Study of Mist Generated from Metalworking Fluids Emulsions. *J. Aerosol Sci.* **2013**, *61*, 70–80. [CrossRef]
20. NSK Ltd. Catalogs and CAD Drawings. NSK Global. Available online: https://www.nsk.com/ctrg/# (accessed on 13 November 2023).
21. Anker, J.E.; Mayer, J.F. Simulation of the Interaction of Labyrinth Seal Leakage Flow and Main Flow in an Axial Turbine. In *Turbo Expo. 2002, Parts A and B*; ASMEDC: Amsterdam, The Netherlands, 2002; Volume 5, pp. 217–224.
22. ASM Handbook Committee (Ed.) *Properties and Selection: Irons, Steels, and High-Performance Alloys*; ASM International: Almere, The Netherlands, 1990; ISBN 978-1-62708-161-0.
23. Kosilova, A.G.; Meščerjakov, R.K. (Eds.) *Spravočnik Technologa-Mašinostroitelja. T. 2*; Mašinostroenie: Moscow, Russia, 2001; ISBN 978-5-94275-015-2.
24. ASM Material Data Sheet. Available online: https://asm.matweb.com/search/SpecificMaterial.asp?bassnum=mq304a (accessed on 13 November 2023).
25. Dassault Systèmes SE Mohr-Coulomb Stress Criterion—2019—SOLIDWORKS Help. Available online: https://help.solidworks.com/2019/english/SolidWorks/cworks/r_mohr-coulomb_stress_criterion.htm?verRedirect=1 (accessed on 13 November 2023).